

# ANTENNAS AND PROPAGATION CONSIDERATIONS FOR ROBUST WIRELESS COMMUNICATIONS IN MEDICAL BODY AREA NETWORKS

W.G. Scanlon\*, G. A. Conway, S. L. Cotton

\*The Queen's University of Belfast, Belfast, UK. w.scanlon@qub.ac.uk

**Keywords:** wearable antennas, radio propagation, wireless networking, channel characterisation.

## Abstract

While antennas and propagation are key concerns for any wireless system, their importance becomes more significant for wearable applications such as medical device networking. The paper discusses the design aims for on-body communications, the effect of antenna-body separation on antenna characteristics and the performance of on-body diversity systems.

## 1 Introduction

It is only relatively recently that radio communications for medical applications has enjoyed widespread attention in the research community, even though “wireless” has been used in some clinical investigations for over 50 years (the swallowable endoradiosonde capsule first appeared in the 1950s [1], albeit without a video camera!). Today, medical body area networks (MBAN) are seen as a key challenge for the wireless communications community (e.g., the IEEE 802.15 BAN-SG) who are focusing on a range of issues including security, power consumption, reliability, capacity, range and error performance. Interestingly, with MBANs the antennas and propagation aspects of the problem can be shown to have a significant effect on all of these important issues. Therefore, in this paper we will present some of our current antennas and propagation research results and how they may be applied to improve the performance of MBANs.

MBAN is simply defined as a network of wearable or body-implanted electronic medical devices. Each ‘node’ communicates using wireless technology such as UHF radio [2] or near-field communications. The medical devices themselves may be self-contained systems such as pacemakers or they may be individual sensors, actuators or controllers creating a distributed system (e.g. visual prosthesis). This functional distinction, along with power consumption considerations has the most influence on the choice of network topology employed, e.g., star, mesh, etc., which in-turn will determine the nature of the point-point links that are considered in this paper. Furthermore, the links may not be line-of-sight (LOS) and the relative positioning of nodes may vary due to respiration and other body movements.

## 2 Antenna Considerations

In a UHF radio-based MBAN it is reasonable to assume that each node will incorporate an integrated RF transceiver and antenna operating in one of the ISM or medical-specific bands (Table 1). Further information on the operating bands may be found in Chapters 8 and 9 of [3]. The use of an integrated antenna is most problematic in the case of medical implants where device volume is tightly constrained and care must be taken to maintain hermetic sealing for biocompatibility. In general, it is desirable in MBAN applications to minimise antenna size whilst retaining sufficient impedance bandwidth to cover the required operating band and bodyworn efficiency (i.e., minimise losses in both body tissue and antenna structure). Furthermore, in wearable scenarios user ergonomics dictate that the antenna and device must be low profile and easily incorporated into a dressing, harness or garment with adequate physical robustness to cope with normal movements.

<i>Ref.</i>	<i>Freq. Range(MHz)</i>	<i>comment</i>
MICS	402.0–405.0	Implants only
MEDS	401.0–402.0 405.0–406.0	Under consideration by US FCC
ISM/433	433.05–434.79	EU only (mainly alarms)
SRD/868	868.0–870.0	EU only
ISM/915	902–928	US only
WMTS	608–614 1395–1400 1427–1432	US only and restricted to hospital / medical facility use
ISM/2450	2400–2500	Usually 802.15 / 802.11 technology

Table 1: Potential MBAN operating frequency bands.

Another important consideration for MBAN applications is the ability to efficiently couple two low-profile, compact nodes that do not have LOS. While the local environment (home, ward, office) multi-path propagation effects may help improve conditions, they certainly cannot be relied on. Therefore, the wearable antennas used must be designed to favourably propagate trapped surface (so called “creeping”) waves present with non-perfect conductors (see Fig. 1). In this way, the body skin-air interface itself is used to guide the signal. This is why the far-field radiation pattern is not

particularly useful when assessing the performance of antennas for on-body communications.

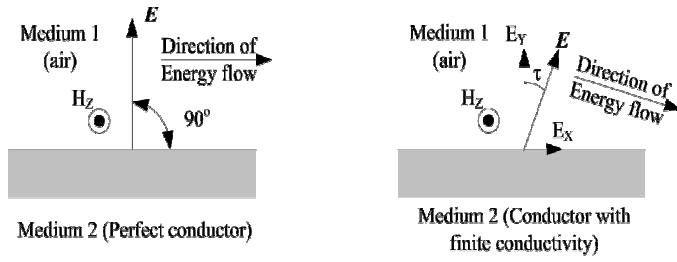


Fig. 1: Trapped surface wave formation on finite conductors.

## 2.1 On-body Antenna Design Example

An example of a low-profile (5 mm) microstrip patch antenna (LP-MPA) suitable for over-the-body-surface communication at 2.45 GHz is presented. Fig. 2 shows the geometry of the LP-MPA antenna with principal dimensions for tissue mounted operation (1 mm separation). A compact ground plane was required to meet the device integration / size requirements mentioned above.

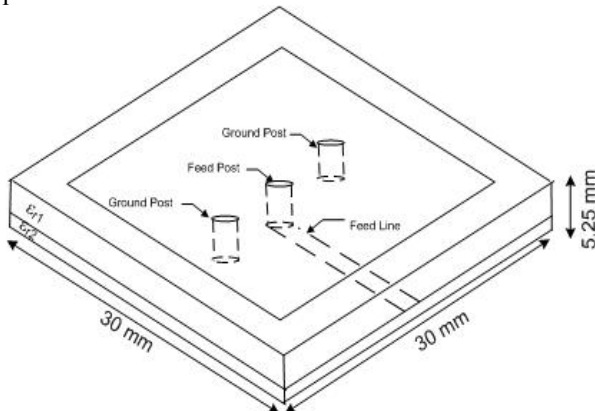


Fig. 2: Geometry of the 2.45 GHz LP-MPA antenna.

The LP-MPA consists of the small groundplane with patch metallization on a dielectric substrate with  $\epsilon_{r1} = 2.33$  (Taconic TLY-3, PTFE woven glass). The antenna is excited at the centre post which is feed by a  $\lambda/4$  microstrip line on a dielectric substrate with  $\epsilon_{r1} = 6.15$  (Taconic RF-60A, PTFE ceramic woven glass). Two posts offset from the feed and shorted to ground are used to force nulls in the tangential electric field component between the groundplane and patch element, exciting a second or higher order resonant mode. It should be noted that the microstrip feed is inherently suitable for device integration and more practical for bodyworn applications.

Using the SEMCAD-X FDTD solver, the antenna groundplane and patch element were modelled as a thin sheet of perfect electrical conductor (PEC) on the relevant dielectric substrate. Both the antenna probe feed and shortening posts were modelled as a thin PEC wire. Rather than a volume representation, a sub-cellular approximation was generated

for thin sheet and wire bodies to give a more accurate representation of the thin structure. Furthermore, a larger minimum cell size could be used, directly improving simulation time. A voltage source (edge source) with an internal resistance of  $50 \Omega$  was used to excite the antenna. For broadband frequency response simulations, a Gaussian sinusoid centred at 2500 MHz with a frequency spectrum from 2 GHz to 3 GHz was used. A non-uniform grid was incorporated in the model to reduce the number of voxel cells required in the computational domain. The maximum cell size near the boundaries of the computational domain was 5 mm ( $\lambda/20$ ). A grid refinement factor of 10 was used on the boundary edges of all solids to ensure appropriate base lines were generated for the model. The minimum cell size in the computational domain was 0.05 mm.

The efficiency, bandwidth and match for the patch antenna were compared with a standard  $\lambda/4$  monopole antenna on the same size of groundplane (modelled as a  $0.24 \lambda$  PEC wire with a diameter of 1.2 mm). Each antenna was modelled with a 1 mm gap from a numerical tissue phantom (see 2.2 below) representing muscle tissue. The results (Fig. 3 and Table 2) show that while the patch antenna performs reasonably well in terms of both efficiency and 10-dB bandwidth, the monopole is significantly better on both counts.

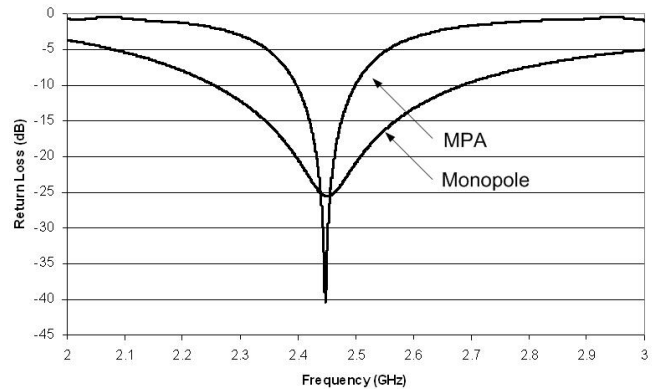


Fig. 3: Simulated  $S_{11}$  return loss for 5mm LP-MPA vs Monopole (1 mm from muscle tissue)

	<i>Monopole</i>	<i>LP-MPA</i>
10-dB bandwidth	430 MHz	103 MHz
Resonant frequency	2450 MHz	2448 MHz
Tissue and dielectric losses	1.49 dB	2.46 dB
Bodyworn efficiency	71 %	56.7 %

Table 2: LP-MPA and monopole antenna characteristics (1 mm from muscle tissue).

## 2.2 On-body Antenna Coupling Performance

On-body (over the body surface) antenna coupling performance is of particular interest in MBAN applications. Clearly there are a large number of scenarios that could be considered in terms of device location, user movement and

the nature of the surrounding multipath environment. However, as mentioned above, it is desirable for an on-body antenna to generate the trapped surface wave rather than have to rely on multipath effects. That way communication between nodes is maintained, regardless of a patient’s particular location or movements. In this section we show how to isolate these surface wave effects from other propagation modes using a specially shaped numerical or physical phantom (Fig. 4) to remove the LOS propagation path. This facilitates the proper investigation and optimization of on-body antennas that clearly cannot be achieved by looking at far-field radiation patterns.

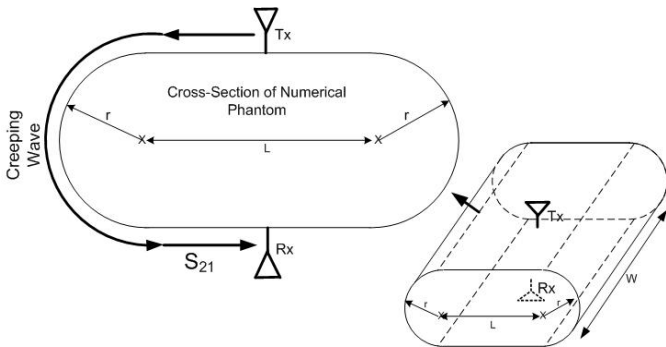


Fig. 4: Phantom design for on-body antenna coupling investigation (see text for specific dimensions).

To investigate the coupling performance of the LP-MPA design in terms of the trapped surface waves the antennas were placed on opposite sides of the cubical-cylinder 3D shaped numerical phantom shown in Fig. 4 with dimensions 100, 50, 400 (L, r, W), respectively. For the 2.45 GHz band, a phantom thickness of 100 mm was chosen to eliminate signal penetration through the volume, effectively isolating the surface propagating mode. Furthermore, the length of the phantom (400 mm) was chosen to reduce any destructive interference effects. Anechoic conditions were represented by the absorbing boundaries in the computational domain. The permittivity and conductivity of the numerical phantom were chosen to represent muscle tissue at 2.445 GHz ( $\epsilon_r = 53.58$ ,  $\sigma = 1.81 \text{ S}^{-1}$ ). The antennas were spaced 1 mm from the numerical phantom. The transmit antenna (Tx) was excited by voltage source (1 V, impedance  $50\Omega$ ). At the receive antenna (Rx) a pure resistive load was placed between the antenna feedpoint and groundplane thus enabling calculation of power delivered to the load from the source ( $S_{21}$ ). An example of the normalized E-field magnitude for the simulation (Fig. 5) shows a number of effects including the wavelength shortening in the tissue, the strong attenuation of the “direct” wave through the tissue and the “creeping” wave produced as the trapped surface wave follows the shape of the air dielectric boundary.

The on-body coupling performance ( $S_{21}$ ) of the LP-MPA is compared to that of the reference monopole antenna (normal to the phantom surface) in Fig. 6. The LP-MPA results are for the three different antenna orientations (broadside, orthogonal and endfire) shown at the bottom of the figure. However, the

LP-MPA orientation had very little influence on the peak  $S_{21}$  values obtained.

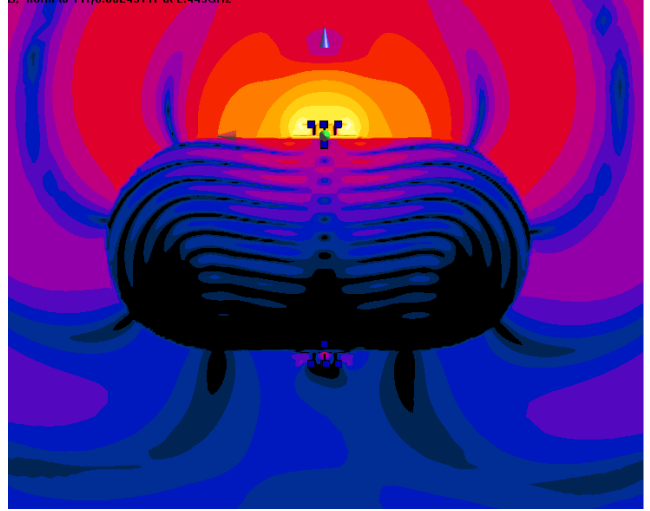


Fig. 5: Simulated LM-MPA normalized E-field magnitude through Tx feedpoint.

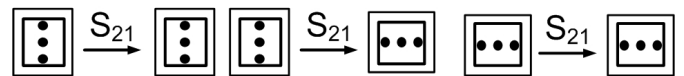
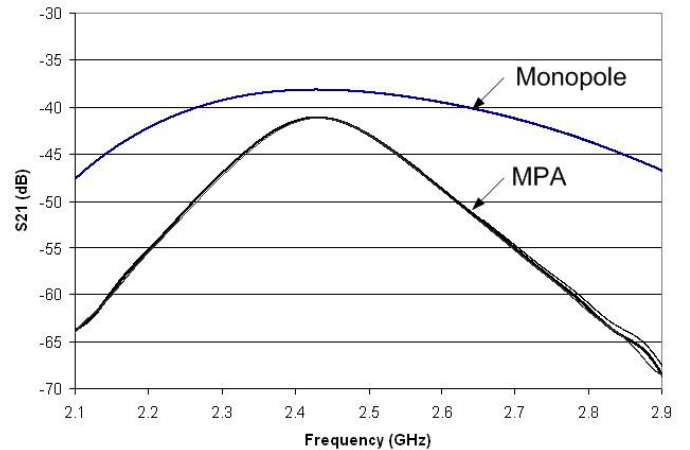


Fig. 6: Simulated  $S_{21}$  coupling loss for LP-MPA Vs Monopole.

The results in Fig. 6 show that while the monopole remains the best choice for on-body NLOS antenna coupling (with a peak  $S_{21}$  of  $-38.2 \text{ dB}$  compared to  $-41.2 \text{ dB}$  for the LP-MPA), the LP-MPA design would be a practical alternative, especially considering that it is  $1/6$  of the height off the body surface. Furthermore, almost  $2 \text{ dB}$  of the  $3 \text{ dB}$  difference in peak  $S_{21}$  values can be attributed to the additional tissue and dielectric losses associated with the patch. The patch also has the advantage of being both compact and robust and has sufficient impedance and coupling ( $3 \text{ dB}$  point) bandwidth for applications in the  $2.45 \text{ GHz}$  band. Nonetheless, there is significant scope to improve on the basic patch design in

terms of reducing both dielectric and tissue losses while maintaining favourable propagating properties.

### 2.3 Measured Antenna-Body Separation Effects

Another important consideration in wearable antenna design is the need for general applicability to the wide range of operational scenarios. While the simulations above are useful for antenna design studies and parameter optimization there is a need to empirically validate the results. In this section we present measurements of return loss and bandwidth for a 10 mm height version of the LP-MPA introduced earlier and demonstrate how performance could be maintained even when the antenna was deployed within clothing rather than a tight fitting harness or medical dressing.

The 10-mm version of the LP-MPA antenna (Fig. 7) consists of a small 30 x 37 mm groundplane and patch metallization on a dielectric substrate with  $\epsilon_{r1} = 2.33$  (Taconic TLY-3, PTFE woven glass). The antenna is also excited at the centre post and feed by a  $\lambda/4$  microstrip line but the substrate here is  $\epsilon_{r2} = 2.33$ . The groundplane was extended by 7 mm to facilitate the mounting of an SMA connector for the measurements. The antenna was initially designed using SEMCAD-X for use with in a measurement scenario with a liquid muscle tissue equivalent phantom where the total separation between the “muscle” and the groundplane was 5 mm. Therefore, they were not fully optimised to be worn on the chest.

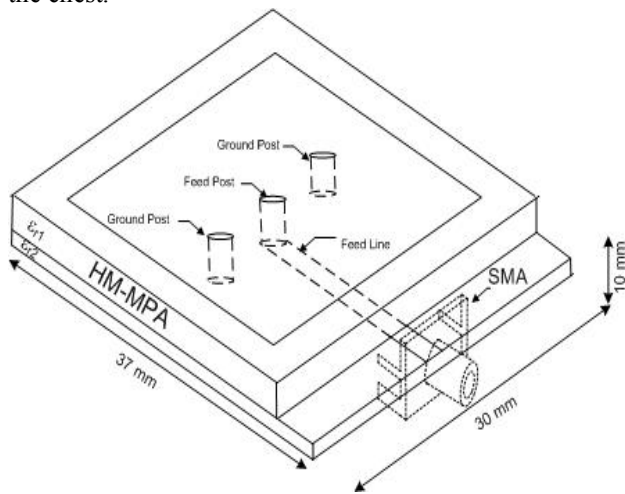


Fig. 7: (a) 10-mm LP-MPA antenna geometry (b) in-situ during  $S_{11}$  measurements with Rhoacell 5-mm foam spacer.

A Rohde & Schwarz ZVB-8 vector network analyser was used for  $S_{11}$  return loss measurements of both the 10-mm LP-MPA and a reference monopole antenna (1.2 mm dia.) on identical groundplanes. The antennas were held close to the chest with various Rhoacell foam ( $\epsilon_r = 1.0$ ) spacers up to 40 mm (Fig. 7(b)). Figure 8 shows how the return loss of the LP-MPA varied with spacing in comparison to the free-space (reference) condition.

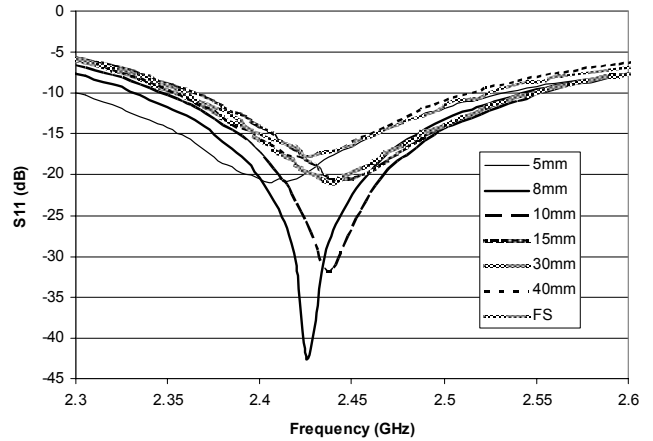


Fig. 8: Measured LP-MPA return loss as function of antenna body separation.

Key data were then extracted from the plots shown in Fig. 8 and from the monopole antenna results (not shown) to examine the effect of antenna-body separation on both resonant frequency and bandwidth. Fig. 9 shows how the monopole antenna resonant frequency was detuned as the antenna was brought closer to the user’s chest, particularly below 30 mm. Note that at around a separation of  $\lambda/4$  (30.5 mm at the centre frequency of 2.45 GHz), the body had a reduced effect on the antenna but this is probably too large and offset for practical MBAN applications. However, the tissue loading increased the  $Q$  of the antenna to improve the bandwidth from 290 MHz in freespace (shown as 60mm on chart) to 650 MHz at 5 mm spacing. The results for the 10-mm LP-MPA (Fig. 10) showed much less antenna interaction effect, albeit against a much lower impedance bandwidth. Nonetheless, the freespace bandwidth of 160 MHz increased to 225 MHz at 5 mm from the chest.

The results in Figs. 8 – 10 were obtained for one volunteer in the lab and in one session and we would expect there to be a small statistical variation if the experiments were to be repeated. Likewise, the body shape and tissue characteristics of the user will have an effect. This is best illustrated in Fig. 11 where the experiment was repeated for the 10-mm LP-MPA mounted close to the head of the same volunteer. The results are not significantly different from those obtained at the chest (Fig. 9) and follow the same trend. This suggests that, in the case of the LP-MPA, the return loss characteristics are dominated by the materials used to construct the antenna rather than the surrounding tissue. Finally, although the

measurements reported here do not include it, it is also important to consider the reduction in antenna efficiency as proximity to the body is reduced.

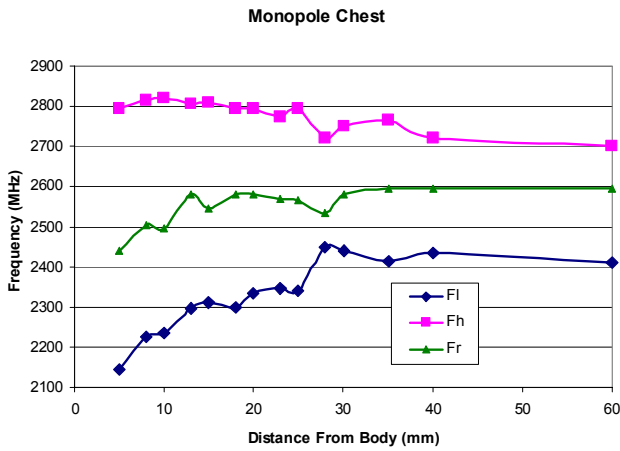


Fig. 9: Measured resonant frequency ( $F_r$ ) and 10-dB points ( $F_h$  and  $F_l$ ) for monopole antenna at chest (note: free-space value shown as 60 mm separation for convenience).

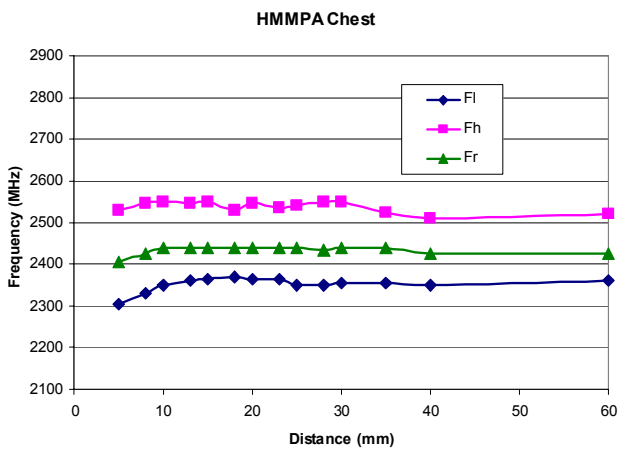


Fig. 10: Measured resonant frequency ( $F_r$ ) and 10-dB points ( $F_h$  and  $F_l$ ) for 10-mm LP-MPA antenna at chest (note: free-space value shown as 60 mm separation for convenience).

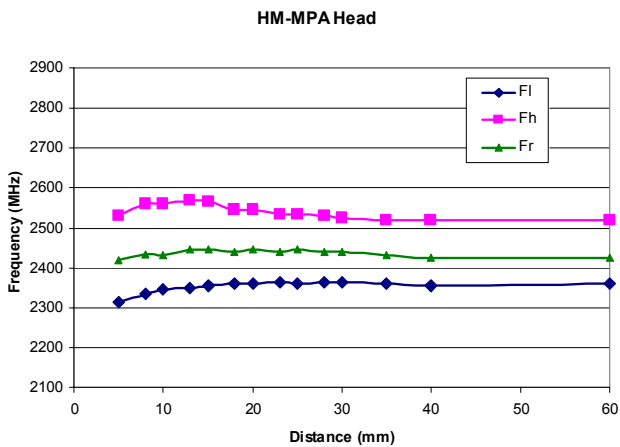


Fig. 11: Measured resonant frequency ( $F_r$ ) and 10-dB points

( $F_h$  and  $F_l$ ) for 10-mm LP-MPA antenna at head (note: free-space value shown as 60 mm separation for convenience).

### 3 Propagation

The results in section 2 suggest that antenna design remains an important issue for on-body communications systems and there are clear gains to be made. However, in the wider sense, system and product engineers cannot tailor their designs for individuals and so they must accept a range of unknown propagation related factors found in real deployments. For example, it is reasonable to assume that some on-body configurations will lead to destructive interference caused by multiple paths over the body surface. While natural body movements such as respiration and, to a lesser degree, environmental multipath effects may reduce the possibility of a “null” it is still important to consider techniques such as spatial diversity. In this section we show that even at relatively low frequencies (such as the 868 MHz ISM band), it is also possible to improve the performance of on-body communications using simple two-branch diversity and, to keep the system as compact as possible, sub-optimal element spacing.

#### 3.1 Real-Time On-Body Diversity Measurements

One of the difficulties in measuring diversity statistics for on-body channels is that even for the most simple scenarios it is impossible to perform “move-and-repeat” type studies due to the uncontrolled random perturbation associated with using live subjects. The only other option is to use off-body instrumentation (such as a multiport vector network analyser) or, as presented here, time-synchronised datalogging receivers at each antenna element. Using a receive signal strength indication (RSSI) recording system described elsewhere [4] we are able to make on-body diversity measurements with any number of antenna elements, limited only in terms of minimum spacing (data logger size) and memory (number of samples). All of the processing is performed off-line based on the time-synchronised RSSI values for each receive antenna.

Fig. 12(a) shows a measured received power profile (256 sa/s) and maximal ratio combining (MRC) time-series for horizontal spatial antenna diversity at 868 MHz while the user was mobile in an open office environment. The receivers (short helical antennas spaced 4 cm,  $0.12\lambda$  apart) were positioned on a volunteer’s left anterior chest with the transmitter on the diagonally opposite back waist. The transmitter was a synthesized RF source equipped with a monopole antenna. Fig. 12(b) shows a time series expansion between 10 and 12 s for clarity. The advantages of MRC diversity are obvious in this case with the elimination of several deep fades.

The cdf for this system (Fig. 13) shows that, for a signal reliability of 90 %, the available diversity gain for MRC was

6.4 dB. Using selection combination (SC) gave 4.9 dB gain with 5.8 dB for equal gain combining (EGC). These diversity gain values would allow for greater on-body range, or perhaps more importantly in MBAN applications, a corresponding reduction in transmitter output power.

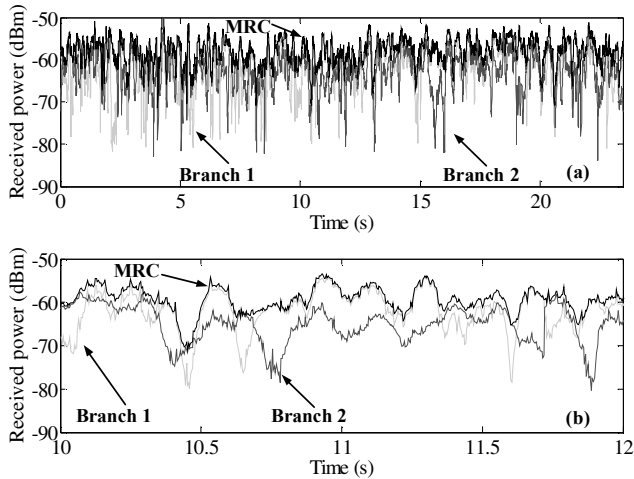


Fig. 12: Received power time-series and related MRC diversity (868 MHz on-body system); (a) 25-s time series, (b) expansion of time series between 10–12 s.

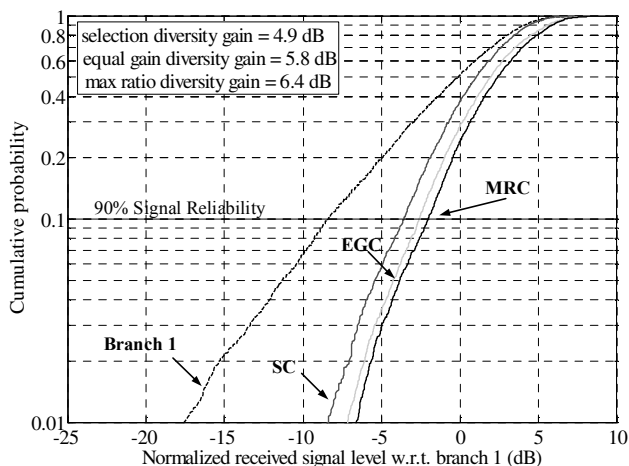


Fig. 13: cdf for 2-branch on-body diversity at 868 MHz.

## 5 Conclusions

Using a number of examples in relevant frequency bands (868 MHz and 2.45 GHz) we have identified a number of important issues for those involved in the design and investigation of on-body radio communications for MBAN applications. The simulated results for the 5-mm patch antenna (LP-MPA) show that design effort should focus on increasing the proportion of radiated power that is propagated as a trapped surface wave to follow the air-tissue interface. Antenna efficiency is another problem that must be carefully considered, especially for compact antennas with dielectric components and where groundplane size is constrained (e.g. in fully integrated devices). Likewise, the measured propagation results highlight that on-body systems would

directly benefit from spatial diversity schemes. However, as the healthcare market is extremely cost conscious and favours “disposable” devices, such an implementation may be inappropriate except in the most exotic of clinical applications.

## 4 Acknowledgements

The authors are grateful to the Northern Ireland Department of Employment and Learning, Taconic International Ltd. and the Engineering and Physical Sciences Research Council (ref. EP/D053749/1) for supporting this work.

## References

- [1] R. S. Mackay, B. Jacobson. “Endoradiosonde”, *Nature*, **45**, pp. 1239–1240, (1957).
- [2] N. F. Timmons, W. G. Scanlon. “Analysis of the performance of IEEE 802.15.4 for medical sensor body area networking,” *1<sup>st</sup> IEEE Comms. Soc. Conf. Sensor & Ad Hoc Communications & Networks (SECON)*, Santa Clara, pp. 16–24, (2004).
- [3] P. S. Hall, Y. Hao (eds.). *Antennas and Propagation for Body-Centric Wireless Communications*. Artech House, Norwood, MA. (2006).
- [4] S. L. Cotton, W. G. Scanlon. “Characterization and modeling of the indoor radio channel at 868 MHz for a mobile bodyworn wireless personal area network.” *IEEE Antennas & Wireless Propagation Letters*, Vol. 6, pp. 51–55, (2007).